Studies on the conformation and dynamics of the C8-substituted guanine adduct of the carcinogen acetylaminofluorene; model for a possible Z-DNA modified structure

Stephen Neidle[1], Reiko Kuroda[1], Suse Broyde[4], Brian E.Hingerty[3], Robert A.Levine[4], Dwight W.Miller[4] and Frederick E.Evans[4]

[1]Cancer Research Campaign Biomolecular Structure Research Group, Department of Biophysics, King's College University of London, London WC2B 5RL, UK

Received 11 September 1984; Revised and Accepted 11 October 1984

ABSTRACT

The structure of an adduct between guanine and the carcinogen acetylaminofluorene has been examined in the solid state by X-ray crystallography, and in solution by NMR techniques. The observed conformations have been compared with predictions from energy calculations and their relevance to models of adducts with DNA has been examined.

INTRODUCTION

The powerful liver carcinogen 2-(acetylamino)fluorene (AAF[1]) is believed to exert its biological effect via metabolism to various reactive species that can bind to cellular macromolecules such as DNA[2-4]. N-esterification has been found to be an important metabolic pathway that can lead to DNA adducts involving attachment at the C8 position of guanine residues[5,6]. It has been proposed that conformational properties of the AAF-bound region in a double-standard DNA molecule may be important factors in the biological responses subsequent to carcinogen binding. In particular, DNA repair which governs tumour initiation[12,13] may be conformation dependent. These conformational aspects are dependent on the nature of the guanine-bound adduct, with AAF and AF (i.e. deacetylated AAF) producing very distinct lesions in DNA structure[9], which correlate with differences in consequent repairibility[7,8,9,10]. The AAF adduct with the polynucleotide poly (dG-dC)· poly (dG-dC) stabilises a Z-DNA structure[12-15,19] more readily than the AF one[8,9]. In random sequence DNA, solution studies suggest that AAF linked to guanine at C8 causes base-displacement[16] or insertion-denaturation[17], while AF is believed to be positioned on the exterior of the double helix[18-20].

Previous studies have examined the conformational and dynamic properties of N-substituted AAF derivatives in solution[21-23], in the solid state[24], and by theoretical methods[25-27]. The present work describes a comparative examination of the C8 bound guanine adduct of AAF(G-AAF), by a combination of solution, solid-state studies and by semi-empirical energy calculations.

MATERIALS AND METHODS

NMR Spectroscopy

^{1}H NMR measurements were carried out at 500 MHz on a Bruker WM500 spectrometer. The sample was dissolved in methanol-d_4 (400µg/ml). Tetramethylsilane (TMS) was added as an internal reference; and chemical shifts are reported in ppm downfield from TMS. Resonance assignments and the barrier to rotation about the amide bond were determined by procedures described previously[21]. Solubility limitations prevented ^{13}C NMR measurements. The mass spectrum was obtained on a Finnigan 4023 mass spectrometer operated in a positive ion chemical ionization mode using ammonia as the reagent gas and a source temperature of 200°C.

For the NMR study, G-AAF was synthesized by acid catalyzed hydrolysis of the sugar moiety from the 8-(N-fluorene-2-yl-acetamido)-2'-deoxyguanosine 5'- monophosphate (dGMP-AAF) adduct. The adduct[23] (10mg) was dissolved in a test tube containing 5ml of 10% isopropanol/water solution. Three drops of 1 M hydrochloric acid were added to the tube which was sealed and heated at 40°C for 24 hours. The resulting precipitate was removed by centrifugation and redissolved in 1ml of 0.05 M sodium hydroxide solution. The solution was neutralized with 0.05 M hydrochloric acid and the precipitate collected. The ^{1}H NMR data (Table I) and the mass spectral molecular ion (M^+=373 m/z) indicated that the product was G-AAF.

X-ray Crystallography

The crystal was grown by a vapour diffusion method from a droplet containing 0.07 mM, dGMP-AAF in 5.7% isopropanol solution. A small thin colourless crystal of dimensions 0.07 X 0.23 X 0.03 mm appeared after ten months. It was kept in a Lindemann quartz capillary tube together with mother liquid for all subsequent diffraction work. Preliminary oscillation and Weissenberg photographs indicated monoclinic symmetry. Accurate cell dimensions were determined from least-squares refinement of 25 θ values measured on an Enraf-Nonius CAD4 diffractometer. Intensity data were collected with Ni-filtered Cu Kα using an ω-2θ scan mode, up to θ = 50°. A periodic check on the intensities of three strong reflections showed that no crystal decay occured during the data collection. The scan width used in the data collection was ω = 1.0 + 0.15 tan θ, with a maximum scan time of 90 s per reflection. A total of 1769 unique reflections were measured, of which only 559 had $I > 1.5\ \sigma(I)$. The merging index between equivalent reflections was 0.11 prior to an absorption correction.

Crystal data: $C_{20}H_{16}N_6O_2$, M.W. = 372.38, Monoclinic,
a = 26.179 (3), b = 9.453 (2), c = 14.253 (1) Å, β = 105.23 (1)°,
V = 3404.3 (15) Å^3, D_c = 1.454 g cm^{-3}, Z = 8, F(000) = 1552,
Space group C2/c, μ(CuK$_\alpha$) = 7.70 cm^{-1} (λ = 1.54051Å).

The structure was solved by direct methods using the program MULTAN 82[28]. The phase set with an outstandingly high combined figure of merit compared to the other sets, of 2.78, was the correct one. This revealed the positions of 23 atoms. Those for the remaining five nonhydrogen atoms were found from difference Fourier syntheses, although difficulties were encountered in the location of two fluorene ring atoms. Scattering factors were taken from 'International Tables for X-ray Crystallography'[29].

The structure was refined by full-matrix least-squares techniques minimising the function $\Sigma w(|F_o| - |F_c|)^2$. Unit weights w were found to produce the smoothest analysis of variance. Due to the low parameter: observation ratio, it was not possible to simultaneously refine positional and individual atomic anisotropic thermal parameters. Hydrogen atom positions were not located in difference electron density maps, so their contributions were included at calculated positions, with isotropic thermal parameters assigned to be the same as that of the atom to which each was bonded. Refinement did not proceed smoothly due to the high thermal motion of several carbon atoms in the unsubstituted phenyl ring of the fluorene group; considerable parameter oscillation was encountered, together with poor intramolecular geometry. Refinement constraining the geometry of the guanine and fluorene rings proved to be the only way of producing acceptable geometry up till the final stages. The situation was improved by the application of empirical absorption and extinction corrections, when cautious full-matrix unconstrained refinement was used and was finally judged to have converged at a conventional R of 0.118 and of 0.121 for the residual defined as $[\Sigma(|F_o| - |F_c|)^2/\Sigma|F_o|^2]$. The largest parameter shift/error at this point was 0.06 and the average was 0.01. Atomic co-ordinates are listed in Table II. Lists of observed and calculated structure factors are available from S.N. Crystallographic calculations were performed with the SDP[30a] and SHELX[30b] computing systems.

Conformational Energy Calculations

The energy of the G-AAF was calculated employing Van der Waals, electrostatic and torsional contributions:

$$E = E_{\text{non-bonded}} + E_{\text{electrostatic}} + E_{\text{torsion}}$$

Potentials and parameters are as described previously for the d(CpG)-AAF adduct[26], with the following change: the torsion barrier for γ was assigned the measured value of 12.3 Kcal mole^{-1} reported below. H9 of G-AAF, which replaces C1' of the deoxy-dinucleoside monophosphate, has a compound charge of 0.1208 (using the INDO method), and an assigned N9-H9 bond length of 1.00Å. Starting conformations (in degrees) were the following combinations: from 0° to 360° in steps of 15°, for angles α and β; 0°, 180° for γ and 60° for δ (where δ is the torsion angle about the NA2 - CA14 - CA15 - H bond). For each of these 1152 trials, the energy was minimised as a function of the conformation by means of the Powell algorithm[31]. Data for the approximately 5 Kcal mole^{-1} contours in Figure 4 were interpolated from the energies of starting conformations.

RESULTS AND DISCUSSION

NMR

The ^{1}H NMR spectrum of G-AAF has been recorded as a function of temperature (Figure 1). At 50°C a conventional time-averaged spectrum is observed (Figure 1a), while at -50°C a complex spectrum comprised of three detectable subspectra of unequal intensity is observed (Figure 1b). Addition of a small amount of base simplifies the low temperature spectrum by reducing the total number of subspectra to two as well as altering the relative intensities (Figure 1c). The spectral parameters (Table I) are characteristic of slow cis-trans isomerism about the amide bond (γ) of AAF compounds[21]. The major conformer is determined to have a trans orientation between the amide oxygen and the fluorene ring (γ≈ 180°) based on the downfield shifts of the fluorene resonances and the upfield shift of the methyl resonance compared to the corresponding resonances of the cis conformer (γ ≈ 0°)[21]. The ratio of cis and trans conformers is 23:77 in the absence of added base. Additional NMR measurements were carried out at -35°C in order to measure the barrier to internal rotation about the amide bond. Complete band shape analysis indicates a barrier of 12.3 ± 0.1 Kcal mole^{-1}.

^{1}H NMR measurements have also been carried out on hypoxanthine under the same experimental conditions as those utilized for G-AAF. Two subspectra are observed which coalesce upon addition of base. Similar studies on the parent compound guanine were prevented by insolubility. However, the results on hypoxanthine can be useful as a model for G-AAF since both are purines containing a keto group at C6. Hypoxanthine is known to undergo N7:N9 tautomerism at an intermediate rate on the NMR time scale[32]. This was observed in the form of resonance broadening in the ^{13}C NMR spectrum

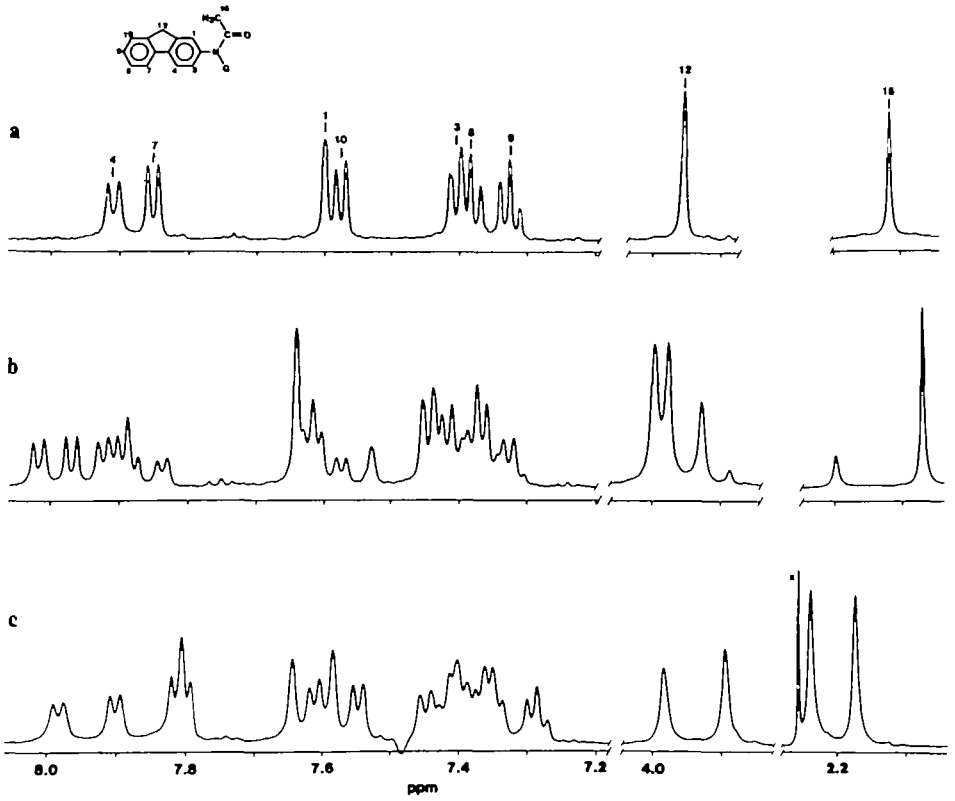

Figure 1. 500 MHz NMR spectrum of G-AAF obtained (a) in methanol-d_4 at 50°C, (b) im methanol-d_4 at -50°C, and (c) in methanol-d_4 with a small amount of sodium hydroxide added at -50°C. Resonance assignments are shown in (a). Spectra were obtained with a 6K sweep width and 32k data points following 200-400 scans. Data were processed using exponential filtering of 0.5 Hz.

recorded at ambient temperature[32]. It is reaonable to conclude that our ^1H measurements at low temperature and in the absence of base enabled detection of both N7 and N9 tautomers of hypoxanthine in slow exchange. These results are similar to those for G-AAF. It is concluded that the multiple subspectra for G-AAF are due to tautomerism and cis-trans isomerism. In the presence of base, the rate of tautomerism is increased such that only two subspectra due to cis-trans isomerism are observable. Rapid rotation about the guanyl-nitrogen (α) and the fluorenyl-nitrogen bond (β) is suggested by the lack of additional subspectra.

The conformation and dynamics of G-AAF in methanol solution has similar-

TABLE I. ^{1}H NMR Chemical Shifts in ppm

Temperature °C	50[a]	-50[b]	-50[b]
Conformation	Ave.	$\gamma = 0^{o}$	$\gamma = 180$
Assignments			
A1	7.60	7.58	7.64
A3	7.40	7.40	7.45
A4	7.91	7.82	7.98
A7	7.85	7.80	7.90
A8	7.38	7.35	7.41
A9	7.32	7.28	7.39
A10	7.58	7.55	7.61
A12	3.96	3.89	3.98
A15	2.12	2.13	2.07

[a] Sample dissolved in methanol-d_4.

[b] Sample dissolved in methanol-d_4 with a small amount of sodium hydroxide added.

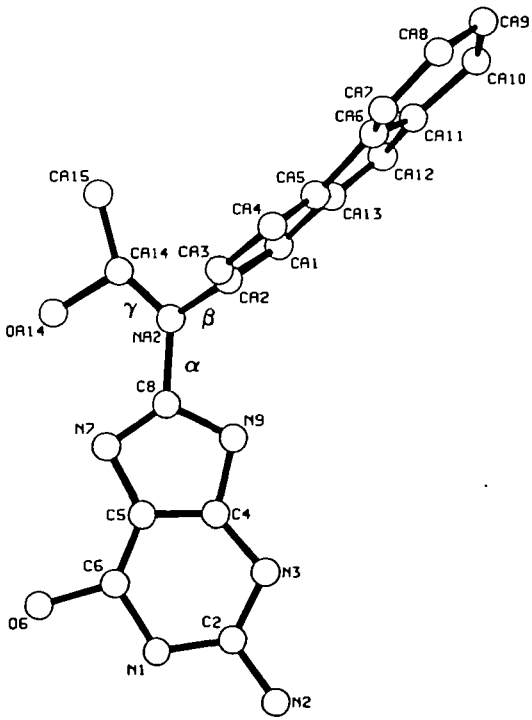

Figure 2. A view of the G-AAF molecular structure as determined by X-ray crystallography.

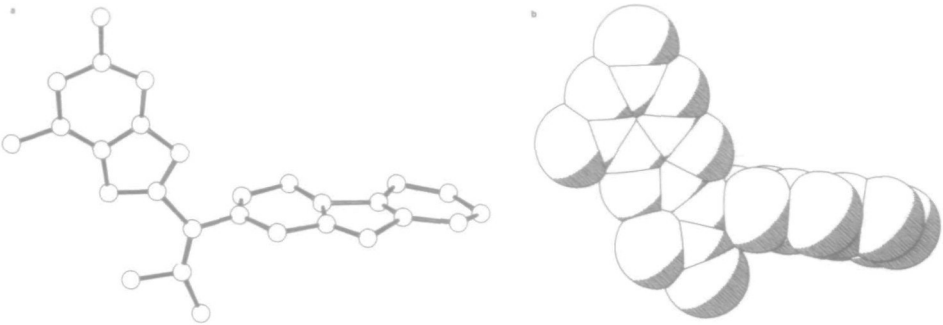

Figure 3. The G-AAF molecular structure viewed along the plane of the fluorene group, (a) in ball-and-stick and (b) in Van der Waals mode. The program PLUTO has been used to produce these figures.

ities to that previously reported for dGMP-8-AAF. Both exhibit a preference for the trans conformer about the amide bond ($\gamma = 180°$), and the barrier to internal rotation about the amide bond computed for G-AAF is in the range previously estimated for the nucleotide adduct[23]. ^{13}C NMR studies on the nucleotide adduct as well as several other N-substituted AAF compounds have indicated that the acetyl group is approximately orthogonal to the fluorene ring (β in the vicinity of 90° or -90°) in solution when γ is near 180°[21,23]. This is consistent with the crystal structure and the theoretical calculation for G-AAF, as well as the earlier prediction for d(CpG)-AAF[26]. The NMR data indicate that there is less orthogonal character when γ approaches an angle of 0° due to π conjugation from the C8 nitrogen to the fluorene ring.

X-ray Crystallography

The structure determination has unequivocally shown that the crystal analysed is of the guanine adduct of AAF, and not of the corresponding nucleotide adduct (Figures 2,3). It is established that acidic conditions promote cleavage of the glycosidic bond in this adduct (see NMR experimental section); however it appears that the prolonged period of crystallisation, even though ostensibly under mild neutral conditions, had produced the same effect.

Bond lengths and angles are listed in Table III. Estimated standard deviations are large, due in large part to the poor ratio of variables to observations, and to low crystal quality. These in turn are mainly ascribable to the large thermal paramerers of atoms CA8 and CA12 in the unsubstituted phenyl ring of the fluorene group, indicating either high thermal motion of this part of the molecule or positional disorder. Examination of

Table II. Unit-cell positional and thermal parameters (in $Å^2$).

(a) Non-hydrogen atoms			
	x	y	z
N1	0.2432	-0.0143	0.2043
C2	0.2349	0.1021	0.2536
N2	0.2486	0.0874	0.3528
N3	0.2113	0.2214	0.2147
C4	0.1970	0.2195	0.1143
C5	0.2053	0.1175	0.0563
C6	0.2253	-0.0035	0.1007
O6	0.2372	-0.1221	0.0603
N7	0.1869	0.1473	-0.0390
C8	0.1698	0.2757	-0.0311
N9	0.1745	0.3303	0.0570
NA2	0.1469	0.3724	-0.1122
CA1	0.1319	0.6187	-0.0959
CA2	0.1117	0.4802	-0.1017
CA3	0.0602	0.4477	-0.1099
CA4	0.0212	0.5480	-0.1084
CA5	0.0387	0.6777	-0.1109
CA6	0.0048	0.8053	-0.1180
CA7	-0.0484	0.8229	-0.1286
CA8	-0.0674	0.9588	-0.1362
CA9	-0.0387	1.0827	-0.1392
CA10	0.0196	1.0597	-0.1177
CA11	0.0365	0.9137	-0.1092
CA12	0.0970	0.8767	-0.1003
CA13	0.0912	0.7236	-0.0967
CA14	0.1411	0.3482	-0.2126
CA15	0.1195	0.4209	-0.2962
OA14	0.1684	0.2288	-0.2168
(b) Hydrogen atoms			
HN1	0.261	-0.102	0.238
HN21	0.244	0.168	0.395
HN22	0.264	-0.004	0.383
HN9	0.164	0.426	0.076
H1	0.170	0.642	-0.092
H3	0.050	0.346	-0.117
H4	-0.016	0.524	-0.106
H7	-0.072	0.740	-0.131
H8	-0.106	0.970	-0.140
H9	-0.056	1.178	-0.154
H10	0.045	1.140	-0.110
H121	0.122	0.916	-0.040
H122	0.109	0.908	-0.158

Fourier maps did not enable a meaningful multi-site partial occupancy model to be developed so thermal disorder may be the likeliest explanation for this effect. Some bond lengths are either too short or too long compared to the known structures of N-OH AAP, 1-OH AAP, 3-OH AAP[27] and guanine[33], and there-

Table III. Bond lengths (Å) and angles (°) and torsion angles (°) with estimated standard deviations in parentheses.

N1	-	C2	1.35(1)			CA1	-	CA13	1.45(3)			
N1	-	C6	1.43(2)			CA2	-	CA3	1.36(2)			
C2	-	N2	1.37(1)			CA3	-	CA4	1.40(2)			
C2	-	N3	1.34(2)			CA4	-	CA5	1.31(3)			
N3	-	C4	1.38(1)			CA5	-	CA6	1.49(3)			
C4	-	C5	1.32(2)			CA5	-	CA13	1.41(3)			
C4	-	N9	1.36(1)			CA6	-	CA7	1.37(2)			
C5	-	C6	1.35(2)			CA6	-	CA11	1.30(3)			
C5	-	N7	1.35(2)			CA7	-	CA8	1.37(3)			
C6	-	O6	1.34(2)			CA8	-	CA9	1.40(4)			
N7	-	C8	1.31(2)			CA9	-	CA10	1.49(4)			
C8	-	N9	1.33(1)			CA10	-	CA11	1.45(4)			
C8	-	NA2	1.47(2)			CA11	-	CA12	1.59(3)			
NA2	-	CA2	1.41(2)			CA12	-	CA13	1.46(3)			
NA2	-	CA14	1.42(6)			CA14	-	CA15	1.36(6)			
CA1	-	CA2	1.41(2)			CA14	-	OA14	1.35(3)			
C2	-	N1	-	C6	115(1)	NA2	-	CA2	-	CA3	119(2)	
N1	-	C2	-	N2	115(1)	CA1	-	CA2	-	CA3	124(2)	
N1	-	C2	-	N3	126(1)	CA2	-	CA3	-	CA4	124(2)	
N2	-	C2	-	N3	119(1)	CA3	-	CA4	-	CA5	112(2)	
C2	-	N3	-	C4	113(1)	CA4	-	CA5	-	CA6	124(3)	
N3	-	C4	-	C5	128(1)	CA4	-	CA5	-	CA13	128(2)	
N3	-	C4	-	N9	125(1)	CA6	-	CA5	-	CA13	108(3)	
C5	-	C4	-	N9	108(1)	CA5	-	CA6	-	CA7	133(3)	
C4	-	C5	-	C6	116(1)	CA5	-	CA6	-	CA11	106(3)	
C4	-	C5	-	N7	114(1)	CA7	-	CA6	-	CA11	121(3)	
C6	-	C5	-	N7	130(2)	CA6	-	CA7	-	CA8	117(2)	
N1	-	C6	-	C5	122(1)	CA7	-	CA8	-	CA9	127(3)	
N1	-	C6	-	O6	110(2)	CA8	-	CA9	-	CA10	114(4)	
C5	-	C6	-	O6	128(2)	CA9	-	CA10	-	CA11	116(4)	
C5	-	N7	-	C8	98(1)	CA6	-	CA11	-	CA10	125(4)	
N7	-	C8	-	N9	119(1)	CA6	-	CA11	-	CA12	116(3)	
N7	-	C8	-	NA2	126(1)	CA10	-	CA11	-	CA12	120(3)	
N9	-	C8	-	NA2	115(2)	CA11	-	CA12	-	CA13	96(2)	
C4	-	N9	-	C8	101(1)	CA1	-	CA13	-	CA5	118(2)	
C8	-	NA2	-	CA2	121(1)	CA1	-	CA13	-	CA12	127(3)	
C8	-	NA2	-	CA14	127(2)	CA5	-	CA13	-	CA12	114(3)	
CA2	-	NA2	-	CA14	109(2)	NA2	-	CA14	-	CA15	135(2)	
CA2	-	CA1	-	CA13	112(2)	NA2	-	CA14	-	OA14	105(4)	
NA2	-	CA2	-	CA1	116(2)	CA15	-	CA14	-	OA14	119(4)	
α (N9	-	C8	-	NA2	- CA2)	-28(3)						
β (C8	-	NA2	-	CA2	- CA1)	108(3)						
γ (C8	-	NA2	-	CA14	- CA15)	178(4)						

fore are not of sufficient accuracy to be discussed in detail. The compound also adopts a trans conformations (γ) about the amide bond.

Both AAF and guanine moieties are planar, within experimental error, and the dihedral angle between the two planes is 95°. A near perpendicular orientation between the fluorene group and guanine was predicted for the d(CpG)-AAF adduct[26]. The acetyl torsion angles are listed in Table II; this

Table IV Minimum Energy Conformations of G-AAF

			$\gamma = 180^{o}$ Region		
Conformer	α	β	γ	δ	ΔE^{a}
1	142	118	159	87	0
2	-143	-118	-159	-87	0
3	144	-62	158	88	0.08
4	-144	62	-158	-88	0.08
5	-32	121	157	90	0.66
6	32	-121	-157	-90	0.66
7	-33	-61	157	89	0.71
8	33	61	-157	-89	0.71
			$\gamma = 0^{o}$ Region		
Conformer	α	β	γ	δ	ΔE
9	-39	127	-23	90	0.14
10	39	-127	23	-90	0.14
11	-131	-125	21	-90	0.17
12	131	125	-21	90	0.17
13	-39	-56	-23	90	0.23
14	39	56	23	-90	0.23
15	-133	56	23	28	0.31
16	133	-56	-23	-28	0.31
17	-48	-97	-15	84	0.48
18	48	97	15	-84	0.48
19	-124	-77	13	-83	0.60
20	124	77	-13	83	0.60
21	125	-104	-14	84	0.63
22	-125	104	14	-84	0.63

[a]The difference between the given and the global minimum, in kcal./mole

group as a whole is virtually coplanar with the guanine base (dihedral angle of 14°), and perpendicular to the fluorene chromophore, with a dihedral angle of 87°. The carbonyl oxygen atom OA14 is cis to the guanine base, and coplanar with it. This together with the short OA14.....N7 distance of 2.57 (1)Å suggest that the observed conformation may be stabilised by a weak electrostatic interaction between these two atoms due to the N7:N9 tautomerism, although a formal full hydrogen bond is not involved.

The conformation of the acetylamino group in G-AAF is at variance with that observed in the crystal structures of hydroxylated AAFs[24]. In these, torsion angles equivalent to β are in the range 172-220°, and those equivalent to γ lie between -5° and 17°. It may be concluded that the conformations observed in these structures, even though they are consistently

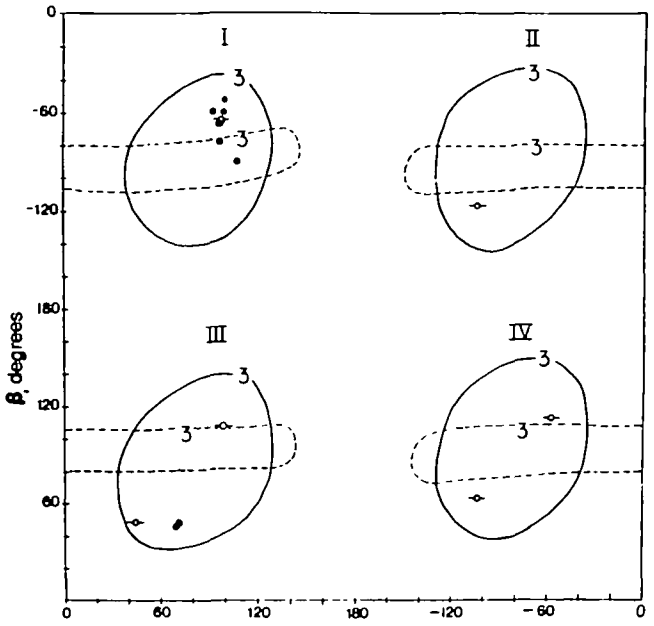

Figure 4. The approximate 5 kcal mole^{-1} contour for G-AAF is indicated by a solid line (———) for $\gamma = 0°$ and by a broken line (-----) for $\gamma = 180°$. (●) designates α,β values of fluorene-cytidine stacked conformers, and (-o-) designates these values in the Z forms, both computed for the guanine C-8-d(CpG) AAF adduct[26,27]. Z-type conformers in regions II and IV were not previously reported.

similar, are not directly relevant to the conformation of AAF when bound to nucleobase. In particular, it is notable that the requirement of coplanarity of acetylamino and fluorene groups in the hydroxylated AAFs, which corresponds to a low energy state, is over-ridden when the side-chain nitrogen atom is bonded to a bulky guanine group. The coplanarity of at least part of a C8-substituted group with the guanine ring has also been observed in the crystal structure of 9-β-D-arabinofuranosyl-8-n-butylaminoadenine[34].

Conformational Energy Calculations

From the 1152 starting conformations, only 22 discrete minima were found, eight for the γ=180° region and fifteen for the γ=0° region. These are listed in Table IV. The conformers occur in pairs of equal energy. The difference in energy between the global minimum and the highest energy conformer is only 0.8 Kcal mole^{-1}, indicating that these forms are all accessible. The actual crystal conformation, with δ set at 60°, is at 2.0 Kcal mole^{-1}, and

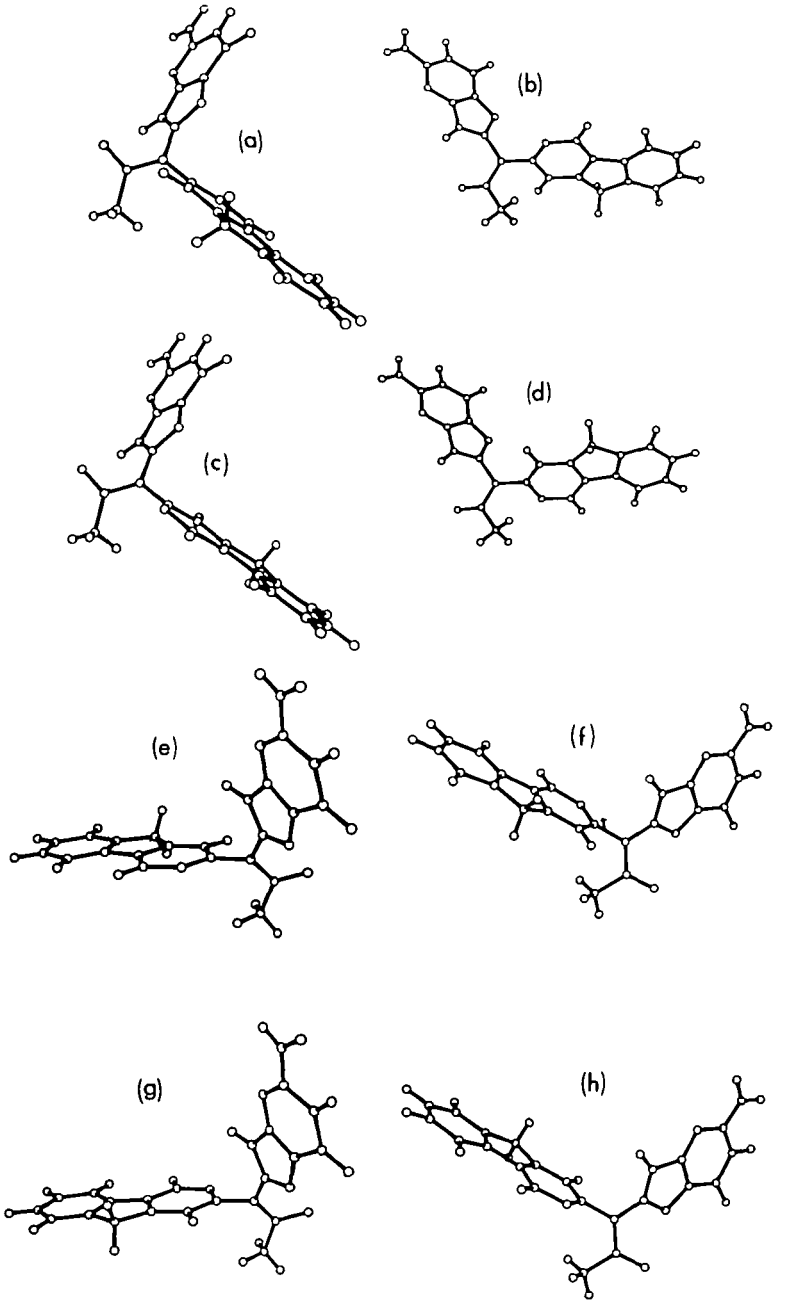

Figure 5. (a)-(h) are conformers 1-8 of Table IV.

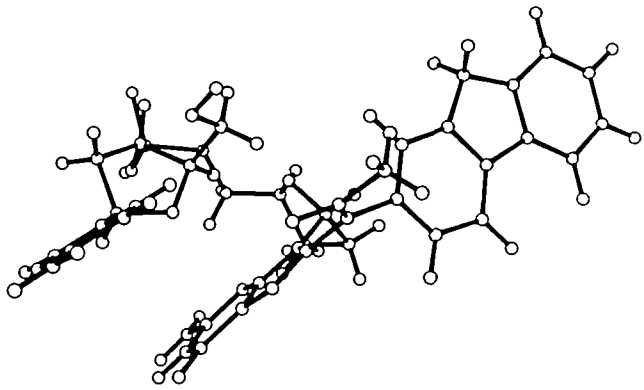

Figure 6. The crystal structure of G-AAF, incorporated into the Z-11 DNA conformation of d(CpG).

the minimum closest to it, namely 5, has an energy of 0.66 Kcal $mole^{-1}$.

Figure 4 shows approximate 5 Kcal $mole^{-1}$ contours for each domain of γ. With $\gamma \sim 0°$, four discrete, nearly symmetrical low energy domains are apparent. These are centered in the vicinity of $\alpha = 90°$, $\beta = 90°$ and span about 60° in each direction. With $\gamma \sim 180°$, β is again centered near 90°, but with a span of about 40°. Within these narrower limits of β, however, α can adopt the entire range of values between about +160° and -160°. Figure 5 illustrates conformers 1-8 of Table IV.

A comparison of these results of G-AAF with those previously computed for the guanine C8 AAF adduct to d(CpG)[26,27], is illuminating. Two types of low energy conformations calculated for deoxydinucleoside monophosphate adducts have been observed in solution. These are forms with fluorene-base stacking [16,17], and Z DNA type conformers[9,12], which place the AAF at the Z helix exterior[26], in a flexible position. The preferred α, β combinations computed for these conformers[26,27] are also shown in Figure 4. The $\gamma = 0°$ region was slightly favoured in both types of conformations, although the energy differency between the two domains was usually less than 1 Kcal $mole^{-1}$. As may be seen in Figure 4, the d(CpG) adduct prefers regions I and III for α, β. The chiral d-deoxyribose interacts differently with the equi-energy G-AAF conformers so that their energies are no longer equal in the larger structure. Furthermore, the constraints of fluorene-cytidine stacking are such that regions II and IV, with α centered near -90° are ruled out. With α near -90° the carcinogen is orientated so that it is swung away from guanine,

instead of being stacked with it, when the DNA backbone conformations are like those reported for fluorene-cytidine stacked forms[26,27]. However, in the Z form the externally located carcinogen can occupy all four domains. Z type conformers in domains II and IV have α, β minima at -102°, -118°; -102°, 64°: and -58°, 116° (data not previously reported). These minima are of somewhat higher energy at the dinucleoside level than the Z type conformers reported earlier[26], but they are entirely feasible forms. The observed crystal structure of G-AAF, with α and β in domain IV is thus a possible fragment of Z-DNA modified at the C8 position of guanine. Figure 6 shows d(CpG) in the Z-II DNA conformation[35], incorporating the crystal structure.

CONCLUSIONS

This study, together with earlier NMR findings on dGMP-AAF[23] and semi-empirical energy calculations for d(CpG)-AAF[26], provides a molecular view of the carcinogen-DNA linkage. The fluorene ring is nearly perpendicular to the base. This crystal structure shows a carcinogen-base orientation that represents one of the possible (though energetically not the most favoured) Z form adduct conformations, with the carcinogen situated in a flexible position at the helix exterior. Thus, the Z form of AAF-bound DNA can be said to arise not merely from a syn glycosidic angle, but from the fundamental features of carcinogen-base orientation.

ACKNOWLEDGEMENTS

This research was supported by grants from the Cancer Research Campaign (S.N. by PHS Grant 1 R01 CA28038-04, awarded by the National Cancer Institute, DHSS (S.B.), DOE Contract DE-AC02-81 ER60015 (S.B.), and by the Office of Health and environmental Research, U.S. Department of Energy, under contract W-7405-eng-26 with the Union Carbide Corporation (B.H.). S.B. thanks Prof. Robert Shapiro for many interesting discussions. We thank Dr. Walter Korfmacher (NCTR) for the mass spectrometry measurements.

[2]Biology Department, New York University, NY 10003, USA

[3]Health and Safety Research Division, Oak Ridge National Laboratory, Oak Ridge, TN 37830, USA

[4]Division of Chemistry, National Center for Toxicological Research, Jefferson, AK 72079, USA

REFERENCES

1. Abbreviations used: AAF, 2-(acetylamino) fluorene: NMR, nuclear magnetic resonance.

2. J.A. Miller and E.C. Miller, "Chemical Carcinogens", C.E. Searle, Ed., ACS Monograph 173, American Chemical Society, Washinton D.C. 1976, pp 737-762.
3. E. Kriek and J.G. Westra, "Chemical Carcinogens and DNA", P.L. Grover, Ed,. CRC Press, Florida, 1979, Vol. 11, pp 1-18.
4. F.A. Beland, W.T. Allaben and F.E. Evans, Cancer res., 40, 834 (1980).
5. E. Kriek, J.A. Miller, U. Juhl and E.C. Miller, Biochemistry 6, 177 (1967).
6. E. Kriek and J.G. Westra, Carcinogenesis 1. 459 (1980).
7. P.C. Howard, D.A. Casciano, F.A. Beland and J.G. Shaddock, Carcinogenesis 2, 97 (1981).
8. P. Rio, B. Malfoy, E. Sage and M. Leng, Environmental Health Persp., 49, 117 (1983)
9. E. Sage and M. Leng, Proc. Natl. Acad. Sci. USA 77, 4579 (1980).
10. F.A. Beland, K.L. Dooley and C. Jackson, Cancer Res., 42, 1348 (1982).
11. M.C. Poirer, B.A. True and B.A. Laishes, Cancer Res., 42, 1317 (1982).
12. R.M. Santella, D. Grunberger, I.B. Weinstein and A. Rich, Proc. Natl. Acad. Sci. USA 78, 1451 (1981).
13. R.M. Santella, D. Grunberger, S. Broyde and B.E. Hingerty, Nucleic Acids Res. 9, 5459, (1981).
14. M. Spodheim-Maurizot, B. Malfoy and G. Saint-Rug, Nucleic Acids Res, 10, 4423 (1982).
15. R.D. Wells, J.J. Miglietta, J. Klysik, J.E. Larson, S.M. Stirdivant and W. Z acharias, J. Biol. Chem. 257, 10166 (1982).
16. D. Grunberger, J. Nelson, C.R. Cantor and I.B. Weinstein, Proc. Natl. Acad. Sci. USA 66, 488 (1970).
17. R.P.P. Fuchs and M. Duane, Biochemistry 11, 2659 (1972).
18. F.E. Evans, D.W. Miller and F.A. Beland, Carcinogenesis 1, 897 (1980).
19. M. Leng, M. Ptak and P. Rio, Biochem. Biophys. Res. Commun. 96, 1095 (1980).
20. R. Santella, E. Kriek, and D. Grunberger, Carcinogenesis 1, 897 (1980).
21. F.E. Evans and D.W. Miller, J. Am. Chem. Soc., 105 4863 (1983).
22. F.E. Evans and D.W. Miller, Biochem. Biophys. Res. Commun. 108, 933 (1982).
23. F.E. Evans and D.W. Miller, Biochem. Biophys. Res. Commun. 108, 933 (1984).
24. S. Neidle, A. Subbiah, A. Mason and S.A. Islam, Carcinogenesis 2, 901 (1981).
25. K.B. Lipkowitz, T. Chevalier, M. Widdifield and F.A. Beland, Chem.-Biol. Interactions 40, 57 (1982).
26. B. Hingerty and S. Boyde, Biochemistry 21, 3243 (1982).
27. Broyde, s. and Hingerty, B. Chem.-Biol. Interactions 47, 69 (1983).
28. S.J. Fiske, S.E. Hull, L. Lessinger, G. Germain, J. -P. Declerq and M.M. Woolfson, MULTAN 82, Universities of York, England and Louvain, Belgium.
29. "International Tables for X-ray Crystallography"; J.A. Ibers and W.C. Hamilton, Eds.: Kynoch Press, Birmingham, 1974; vol. IV.
30. (a) SDP Program System; Ed. B.A. Frenz; inc., College station, Texas, and Enraf-Nonius, Delft, Holland.
(b) The SHELX Program system; author G.M. Sheldrick, Gottingen, Germany.
31. M.J.D. Powell, Computer J. 7, 155 (1964).
32. M.-T. Chenon, R.J. Pugmire, D.M. Grant, R.P. Panzica and L.B. Townsend, J. Am. Chem. Soc. 97, 4636 (1975).
33. D. Voet and A. Rich, Prog. Nucleic Acid Res. Mol. Biol. 10. 153 (1970).
34. S. Neidle, Mr. R. Sanderson, A. Subbiah, J.B. Chattopadhyaya, R. Kuroda and C.B. Reese, Biochem. Biophys. Acta. 565, 379 (1979).
35. A.H.J. Wang, G.J Quigley, F. Kolpack, G. van der Marel, J.H. van Boom and A. Rich, Science 211, 171 (1980).